

Vertical segregation of age-0 and age-1+ polar cod (*Boreogadus saida*) over the annual cycle in the Canadian Beaufort Sea

Maxime Geoffroy¹ · Andrew Majewski² · Mathieu LeBlanc¹ · Stéphane Gauthier³ ·
Wojciech Walkusz² · James D. Reist² · Louis Fortier¹

Received: 2 March 2015 / Revised: 12 September 2015 / Accepted: 12 October 2015 / Published online: 22 October 2015
© Springer-Verlag Berlin Heidelberg 2015

Abstract The offshore marine ecosystem of the Canadian Beaufort Sea faces the double pressure of climate change and industrialization. Polar cod (*Boreogadus saida*) is a pivotal forage species in this ecosystem, accounting for 95 % of the pelagic fish assemblage. Its vertical distribution over the annual cycle remains poorly documented. Hydroacoustic records from 2006 to 2012 were analysed to test the hypothesis that age-0 polar cod segregate vertically from larger congeners. Trawls and ichthyoplankton nets validated the acoustic signal. Fish length, weight, and biomass were estimated from new regressions of target strength and weight on standard length. Polar cod were vertically segregated by size in all months, with small age-0 juveniles in the epipelagic (<100 m) layer and larger age-1+ deeper in the water column. From December to March, the biomass of age-1+ peaked in a mesopelagic layer between 200 and 400 m. With increasing irradiance from April to July, the mesopelagic layer deepened and extended

to 600 m. Starting in July, age-0 polar cod formed an epipelagic scattering layer that persisted until November. From September onward, age-0 left the epipelagic layer to join small age-1+ in the upper mesopelagic layer. Low biomass in the mesopelagic layer from February to September likely resulted from large polar cod settling on the seafloor to avoid diving marine mammals. Longer ice-free seasons, warmer sea-surface temperatures, or an oil spill at the surface would likely impact epipelagic age-0, while mesopelagic age-1+ would be vulnerable to an eventual oil plume spreading over and above the seafloor.

Keywords Vertical distribution · Ontogenic migrations · Acoustics · Target strength · Diel vertical migrations

Introduction

Comprising over 95 % of the pelagic fish assemblage, polar cod (*Boreogadus saida*) is by far the most abundant fish in Arctic seas (Benoit et al. 2008; Fortier et al. 2015). Age-1+ polar cod are ubiquitous in Arctic waters and have been observed in shallow coastal zones, in anfractuosités in sea ice, at depth on the continental slope, and under the ice offshore up to the North Pole (e.g. Welch et al. 1993; Gradinger and Bluhm 2004; Benoit et al. 2010; Mecklenburg et al. 2011; David et al. in press). In the Beaufort Sea, the polar cod ecosystem faces climate change and, potentially, an increased risk of oil spills from exploration drilling and increased navigation (Fortier et al. 2015). The duration of the ice-free season has lengthened in the region since the beginning of the century (Stroeve et al. 2012), and the edge and slope of the Mackenzie shelf are targeted for oil exploration. Documenting the offshore autecology of polar cod over the annual cycle is critical to anticipate the

This article belongs to the special issue on the “Ecology of Arctic Gadids”, coordinated by Franz Mueter, Jasmine Nahrgang, John Nelson, and Jørgen Berge.

Electronic supplementary material The online version of this article (doi:10.1007/s00300-015-1811-z) contains supplementary material, which is available to authorized users.

✉ Maxime Geoffroy
maxime.geoffroy.1@ulaval.ca

¹ Québec-Océan, Département de Biologie, Université Laval, 1045 Avenue de la Médecine, Québec, QC G1V 0A6, Canada

² Freshwater Institute, Fisheries and Oceans Canada, 501 University Crescent, Winnipeg, MB R3T 2N6, Canada

³ Institute of Ocean Sciences, Fisheries and Oceans Canada, 9860 West Saanich Road, PO Box 6000, Sidney, BC V8L 4B2, Canada

impacts of climate change and anthropogenic activities on the slope ecosystem.

Early acoustic surveys and visual observations during the ice-free season showed polar cod to occur primarily as widely dispersed individuals or, occasionally, in dense schools in shallow coastal waters (e.g. Welch et al. 1992; Crawford and Jorgenson 1993; Welch et al. 1993). Based on a simple trophodynamics model, Welch et al. (1992) calculated that, in the Canadian Archipelago, the biomass of polar cod observed nearshore was *circa* 32 times too low to satisfy the requirements of its marine mammal and seabird predators and predicted that large aggregations existed elsewhere. Recent studies in the Beaufort Sea confirmed that age-1+ polar cod form dense aggregations at depth in deep embayments, canyons, and over the continental slope, during the ice-free season in August (Parker-Stetter et al. 2011) and September (Crawford et al. 2012), during the consolidation of the ice pack in October and November (Benoit et al. 2014), and under the consolidated ice cover from December to April (Benoit et al. 2008; Geoffroy et al. 2011). The offshore distribution of adult polar cod in late spring and summer (May–July) and variations in biomass over the annual cycle remain to be described.

In Arctic seas influenced by large rivers, such as in the Canadian Beaufort Sea, polar cod hatch in the surface layer from January to July, often well before the maximum availability of their zooplankton prey (Bouchard and Fortier 2011). At around 30 mm in length, the young fish metamorphose into adult-like age-0 juveniles and start moving deeper in the water column (Ponomarenko 2000). Polar cod are cannibalistic, the adult stages feeding occasionally on the younger stages (e.g. Benoit et al. 2010; Rand et al. 2013). It has been hypothesized that early hatching enables the young fish to reach a minimum size and the capacity to avoid predators before they join their cannibalistic congeners in the deep Atlantic Layer to overwinter (Bouchard and Fortier 2011). If offshore adult cod remain at depth throughout the year including the May–July period, larvae and age-0 juveniles distributed in the surface layer from January to October would effectively be protected from cannibalism until they migrate to depth in October. Alternatively, Geoffroy et al. (2011) hypothesized that age-1+ polar cod leave their deep winter refuge in spring to follow zooplankton prey such as the copepods *Calanus hyperboreus* and *Calanus glacialis* as they ascend to the surface layer to graze on ice algae and phytoplankton. If so, the planktonic stages of polar cod would be vulnerable to cannibalism during spring–summer.

In this study, we test the hypothesis that age-0 and age-1+ polar cod are segregated vertically until the fall migration of the age-0 juveniles from the surface layer to depth. Acoustic records from 2006 to 2012 in the Canadian

Beaufort Sea are combined to document the offshore vertical distribution of polar cod size and biomass over the annual cycle. In particular, we document the summer–fall vertical migration of pelagic age-0 juveniles between July and mid-October and estimate size and biomass from new regressions of target strength (TS; dB re: 1 m²) on standard length (SL) and wet weight (W) on SL.

Materials and methods

Study area and survey design

In 2006 and from 2009 to 2011, the icebreaker CCGS *Amundsen* conducted acoustic surveys in late summer and in the fall in the Canadian Beaufort Sea as part of her annual scientific mission to the Arctic (Fig. 1). Acoustic data were also recorded continuously from October 2007 to August 2008, as the icebreaker navigated the ice pack of the Amundsen Gulf during the Circumpolar Flaw Lead System Study (Geoffroy et al. 2011). In 2012, acoustic transects across the Mackenzie shelf and over the slope from 20 to >1000 m were conducted from the fishing vessel F/V *Frosti* (Fig. 1). The surveys generally took place in summer and autumn (July–October; Table 1). Over the years, the surveyed area covered roughly 415,500 km² (Fig. 1).

Three water layers are superimposed in the Canadian southern Beaufort Sea: (1) the surface Polar-Mixed Layer of variable temperature (PML; <20 m in summer and <40 m in winter, $S < 31.6$); (2) the cold intermediate Pacific Halocline (PH; ~40–200 m, $32.4 < S < 33.1$, $-1.6\text{ }^{\circ}\text{C} < T < 0\text{ }^{\circ}\text{C}$); and (3) the relatively warm deep Atlantic Layer (AL; >200 m, $T > 0\text{ }^{\circ}\text{C}$) (Carmack and Macdonald 2002; McLaughlin et al. 2011). Conductivity–temperature–depth (CTD) systems regularly deployed from the *Amundsen* (SBE-911 plus[®]) and the *Frosti* (SBE-25 and SBE-19plusV2[®]) provided the temperature and salinity profiles used to determine the coefficient of sound absorption (Francois and Garrison 1982) and sound speed (Mackenzie 1981) for acoustic calculations.

Hydroacoustic sampling

Hydroacoustic data at 38 and 120 kHz were continuously recorded on both ships thanks to hull-mounted Simrad EK60[®] split-beam echosounders with 7° acoustic beams. Except for 2009, the systems were calibrated annually by the standard sphere method (Simmonds and MacLennan 2005). Acoustic data collected in 2009 were not pooled with the other years for the monthly TS and biomass calculations. Pulse duration was set at 1024 μs, and ping rate varied from 1 to 2 s (see Benoit et al. 2008; Geoffroy et al.

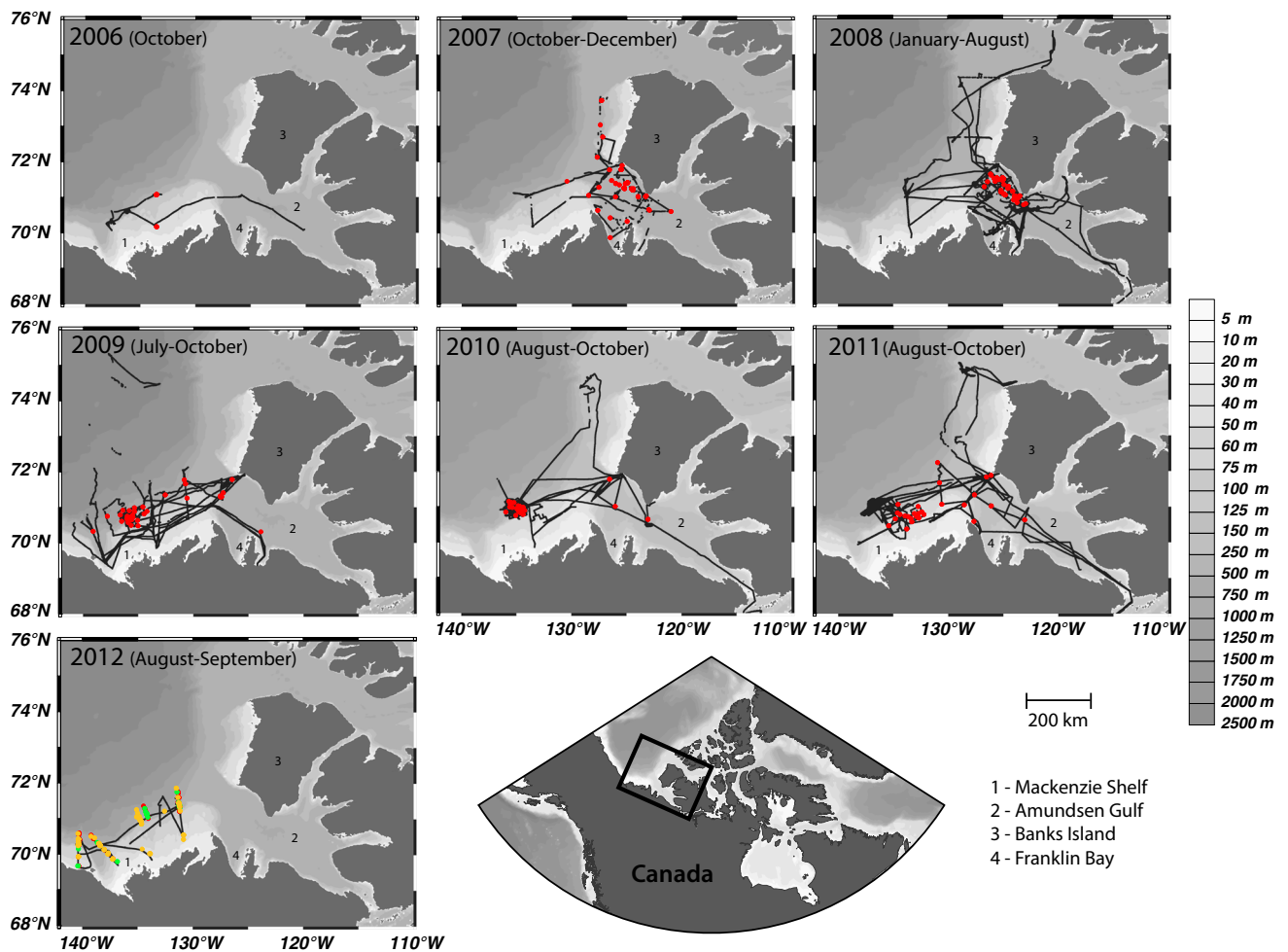


Fig. 1 Bathymetric map of the study area with ship track (black line) and periods surveyed in each year. Red dots ichthyoplankton net tows; green dots mid-water trawls; yellow dots demersal trawls

Table 1 Sampling periods, number of ichthyoplankton net and trawl deployments, and number of polar cod sampled in the epipelagic (0–100 m) and mesopelagic (200–600 m) layers by year

Year	Start date	End date	Nets	Mid-water trawls	Demersal trawls (200–600 m)	Polar cod 0–100 m	Polar cod 200–600 m
2006	10 October	16 October	3	0	0	68	0
2007	15 October	31 December	24	0	0	29	0
2008	1 January	8 August	58	0	0	4002	0
2009	16 July	16 October	42	0	0	2073	0
2010	14 August	8 October	21	0	0	394	0
2011	12 August	3 October	25	0	0	684	0
2012	6 August	3 September	44	21	27	1579	5983

2011 for details). Power was set to 2 kW at 38 kHz and 500 W at 120 kHz, except in 2012 when the power at 120 kHz was reduced to 250 W.

In 2011, a Simrad SX90[®] fisheries sonar mounted in the hull of the *Amundsen* was operated over 1418 km across

bathymetric areas ranging in bottom depth from 20 to >1000 m. Operating frequencies varied from 20 to 30 kHz by 1 kHz increment. This sonar can detect fish schools in the surface layer (0–50 m) within a radius of up to 2 km around the ship (Geoffroy et al. 2015).

Fish sampling and processing

Age-0 (fish larvae and juveniles hatched in the sampling year) and age-1+ fish were sampled to validate the acoustical signal and calculate the regressions of TS on SL and W on SL for size and biomass estimations (Fig. 1, Table 1). A double-square net bearing two square-conical nets (1-m² aperture, 500- μ m mesh) and a rectangular mid-water trawl (8-m² aperture, 1600- μ m mesh) were deployed from the *Amundsen* on 173 occasions between 2006 and 2011 to sample age-0 fish (details in Bouchard and Fortier 2011). In 2012, 44 ichthyoplankton samples were collected with a bongo net (0.25-m² aperture, 500- μ m mesh) deployed from the *Frosti* (details in Walkusz et al. 2013). Sampling depth varied from the surface to between 15 and 100 m from 2006 to 2011, and to between 55 and 350 m in 2012. Ichthyoplankton net deployments were distributed over the study area (Fig. 1). Double oblique tows were conducted on some occasions to increase the catch. Up to 25 polar cod larvae and juveniles per deployment were photographed against a millimetre paper background and measured fresh at sea. Being too light for accurate weighing at sea, small fish were placed on blotting paper for \sim 30 s and inserted individually in commercial Ziploc[®] sealable plastic bags pre-weighed on a \pm 0.001-g precision balance and frozen at -80 °C. In the laboratory, each bag containing a fish was thawed, dried, and re-weighed on the same balance, and the weight of the pre-weighed bag was subtracted to obtain W. Weighted larvae and juveniles as small as 0.9 cm SL sampled in the eastern Canadian Arctic in July and August 2013 were added in the regression of W on SL to increase the range of values.

The trawler *Frosti* sampled age-1+ polar cod in 2012 (Fig. 1). Four subsurface tows (<40 m) were conducted with an Enzenhofer and Hume mid-water trawl (3 \times 3 m aperture; codend mesh = 0.63 cm). A larger Cosmos-Swan 260 mid-water otter trawl (headrope = 41.4 m, 1.27-cm codend mesh, Thyborøn Type 2 Standard 5.12 m² steel doors) was deployed on 17 occasions at water depths ranging from 38 to 420 m, including four casts at depths < 65 m. The mid-water trawls were towed at 3 knots for 20–25 min. Demersal polar cod were sampled with a modified Atlantic Western IIA (headrope = 22.86 m, footrope = 21.23 m, 1.27-cm codend mesh, Thyborøn Type 2 Standard 5.12 m² steel doors) and a beam trawl (headrope = 4.27 m, footrope = 4.27 m, 0.95-cm codend mesh). Adult fish were initially identified to the lowest taxonomic level possible, and polar cod from a random subsample were measured and weighted fresh before freezing at -50 °C for the later confirmation of identification in the laboratory.

Hydroacoustic data processing

For consistency, the acoustic data collected from the *Frosti* and the *Amundsen* were processed with the same protocol using Echoview[®] 5.3. The echograms were visually scrutinized to correct bottom detection by the sounder and to discard noise and signals from other deployed instruments. The top 13.5 m of the water column and the first metre above the bottom were excluded from the analysis. Time-varied gain (TVG) profiles were inserted based on the average sound speed (c in m s⁻¹) and absorption coefficient (α in dB m⁻¹) calculated from the closest CTD cast. A time-varied threshold (TVT = $20\log R + 2\alpha R - 140$, where R is the range from the transducer) was added in the 38 and 120 kHz echograms to offset noise amplification at depth by the TVG.

High fish densities sometimes result in multiple target detections, which overestimate target strength (TS), fish size, and biomass (Sawada et al. 1993; Gauthier and Rose 2001). TS analysis was conducted on the 38-kHz data using the Echoview single-echo detection algorithm for split-beam echosounder (method 2: threshold applied on targets after compensation for their position in the beam) followed by the application of the Echoview fish-tracking algorithm (e.g. Benoit et al. 2014). The fish-tracking algorithm identifies and retains only single echoes that can be tracked over several pings, thus filtering out most superimposed echoes from multiple targets. As a starting point, the parameterization of the two algorithms was set as recommended in previous studies (Parker-Stetter et al. 2009; Rudstam et al. 2009; Benoit et al. 2014). A minimum TS threshold varying from -80 to -65 dB excluded most zooplankton targets. For each day, this threshold was defined as the limit between the lowest two TS distributions corresponding to zooplankton and fish, respectively (Fig. 2). An upper threshold of -43 dB (corresponding to a 35-cm polar cod based on Eq. 1) was used to avoid including the signal of any larger fish species potentially occurring in the area. The parameters for the two algorithms (given in Online Resources 1 and 2) were then further fine-tuned to minimize multiple target detections by reducing the number of outliers at the upper end of the resulting TS frequency distribution.

To validate that our approach limited multiple target detections, TS estimated using the fish-tracking algorithm were compared to TS estimated using the Sawada Index, a recognized approach to minimize multiple target detections (Sawada et al. 1993; Gauthier and Rose 2001). In this approach, TS are calculated only within regions of the echogram with a Sawada Index (number of fish in effective reverberation volume) \leq 0.04, where the probability of multiple target detections is low. The comparison was

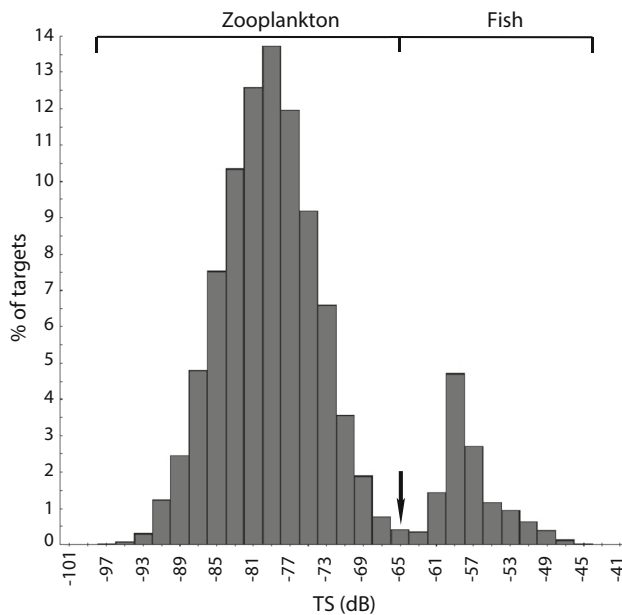


Fig. 2 Example for 12 October 2006 of the daily TS frequency distributions used to determine the minimum threshold for TS analysis, indicated by the arrow. In this case, TS < 65 and >65 dB are attributed to zooplankton and fish, respectively

conducted for echograms recorded over one full week in winter (March 2008) and summer (August 2012).

Locations where age-0 and age-1+ polar cod represented >90 % of catches in ichthyoplankton nets or mid-water trawls were used to calculate the regression of TS on SL (Parker-Stetter et al. 2011). For ichthyoplankton net deployments, TS of all fish detected from 13.5 m to the maximum sampling depth of the net for a period covering approximately 1 h around net deployment were averaged (in m^2 and thereafter transformed in dB). The same method was used for age-1+ polar cod sampled by mid-water trawls in 2012, except that only the TS of fish within ± 25 m depth range of the sampling depth were averaged to prevent the inclusion of different length classes, as polar cod tend to stratify vertically by length (Benoit et al. 2014). Ichthyoplankton net deployments deeper than 200 m and trawl net deployments shallower than 200 m were discarded from the TS analysis to prevent any bias resulting from the selectivity of the different samplers. Stations where the echosounder did not successfully detect individual fish were also discarded. A linear regression of mean TS on \log_{10} of the mean SL of polar cod sampled in the corresponding hauls was then calculated to transform the backscatter signal into fish size (Foote 1987; Simmonds and MacLennan 2005).

Estimation of biomass

The echograms were gridded in echo-integration cells 0.25 nm long by 3 m deep. The difference in mean volume

backscattering strength (ΔMVBS) between corresponding echo-integration cells at 120 and 38 kHz was used to discriminate pelagic fish from aggregations of large zooplankton (e.g. Geoffroy et al. 2011). Minimum and maximum thresholds of $\Delta\text{MVBS}_{120-138}$ were, respectively, set to -10 and 5 dB to isolate the signal of polar cod (Benoit et al. 2014). Echo-integration cells with a volume backscattering strength (S_v ; dB re: 1 m^{-1}) above -40 dB, which is above the maximum S_v of the densest winter aggregations observed, were discarded from the analysis as they likely resulted from bottom or noise detections that were not identified during visual inspection.

Mid-water trawls were deployed in August and early September only. Hence, mean acoustic TS rather than trawl catches was used to estimate biomass and its vertical distribution over the annual cycle. Because the size of pelagic polar cod increases with depth (Benoit et al. 2008, 2014), for each year, the monthly mean acoustic TS (in m^2 and thereafter transformed in dB) was calculated for successive 50-m strata from the surface downward. The density of polar cod (ρ_v in fish m^{-3}) within each 3-m-deep echo-integration cell was then estimated from the mean detected TS value for each stratum using the nautical area backscattering coefficient (NASC in $\text{m}^2 \text{ nm}^{-2}$) at 38 kHz (Parker-Stetter et al. 2009):

$$\rho_v = \frac{\text{NASC}}{4\pi \times 10^{\frac{\text{TS}}{10}} \times 1852^2 \times 3}$$

A regression of wet weight (W in g) on SL (cm) for 5860 polar cod sampled in nets, mid-water trawls, and demersal trawls was calculated in the form $\log_{10}(W) = a_f + b_f \cdot \log_{10}(\text{SL}) + \varepsilon$ to reduce the variance at larger sizes. The residual value ε was assumed to be normal i.i.d., and a_f and b_f are constants for one species. The regression was thereafter transformed in the more standard form $W = a_f \cdot \text{SL}^{b_f}$ (Simmonds and MacLennan 2005). The regression of TS on SL allowed estimating the size of the average fish within each 50-m-deep stratum and was combined with the new regression of W on SL to estimate the weight of the average fish within each stratum. Mean polar cod biomass (B in $\text{g} \cdot \text{m}^{-3}$) within each echo-integration cell was then estimated:

$$B = \rho_v \cdot W$$

As no single target could be detected beyond 600 m, the average TS for the 550–600 m layer was used to estimate polar cod biomass in the deeper layers.

Inter-annual variability

For each month, acoustic records from all years (except 2009 because the echosounder was not calibrated) were combined to document the vertical distribution of polar cod

TS and biomass over the annual cycle. To assess inter-annual variability, the mean monthly TS in each 50-m-deep stratum was compared (one-way ANOVA and Tukey's honest significant difference test) among years for those months sampled in more than 1 year (July, August, September, and October; Table 1). Residuals for the month of August were not normally distributed, and a nonparametric Kruskal–Wallis test was used.

Results

An epipelagic layer of age-0 and a mesopelagic layer of age-1+ polar cod

The overwintering expedition of the *Amundsen* in 2007–2008 provided a near-complete annual record of the vertical distribution of pelagic fish in SE Beaufort Sea from mid-October 2007 to early August 2008 (Table 1). Two distinct scattering layers were observed: an epipelagic layer within the 0- to 100-m depth interval and a mesopelagic layer distributed primarily in the 200- to 600-m interval (Fig. 3). The 217 ichthyoplankton nets deployed within the epipelagic layer (<100 m) from 2006 to 2012 captured 7334 age-0 polar cod (Fig. 4a) that represented 93 % of the

7899 fish sampled. The 8 mid-water trawl hauls in the 0- to 100-m layer captured 1506 fish, which included 1486 age-0 polar cod <5.5 cm and nine age-1 polar cod 5.5–7.5 cm long (Fig. 4b). No age-2 + polar cod (>9 cm) were sampled in the epipelagic layer. The remainder of the epipelagic fish assemblage included the early stages of benthic fish species, mainly Liparidae and Cottidae. Polar cod also dominated the nearly monospecific mesopelagic layer. Ninety-five % of the 1142 fish captured between 200 and 420 m in 13 mid-water otter trawl deployments were polar cod 2.5–16.3 cm long (Fig. 4c). The 27 demersal trawls deployed over bottom depths ranging from 200 to 600 m yielded 4899 polar cod 3.1–21.8 cm long (Fig. 4d).

The epipelagic layer was absent or weak from January to early May, started to form in mid-May, and was fully developed by early August (Fig. 3). By then, age-0 polar cod exhibited clear diel vertical migrations (DVM) within the PML, distributing around 50 m depth in daytime and moving closer to the surface at night (Fig. 3, red outline). From late August to early October, the amplitude of the DVM increased, taking some age-0 polar cod beyond the 100 m depth into the PH and, ultimately, in contact with the mesopelagic layer of age-1+ polar cod (outlined in Online Resource 3). By December, the epipelagic layer had disappeared (Fig. 3).

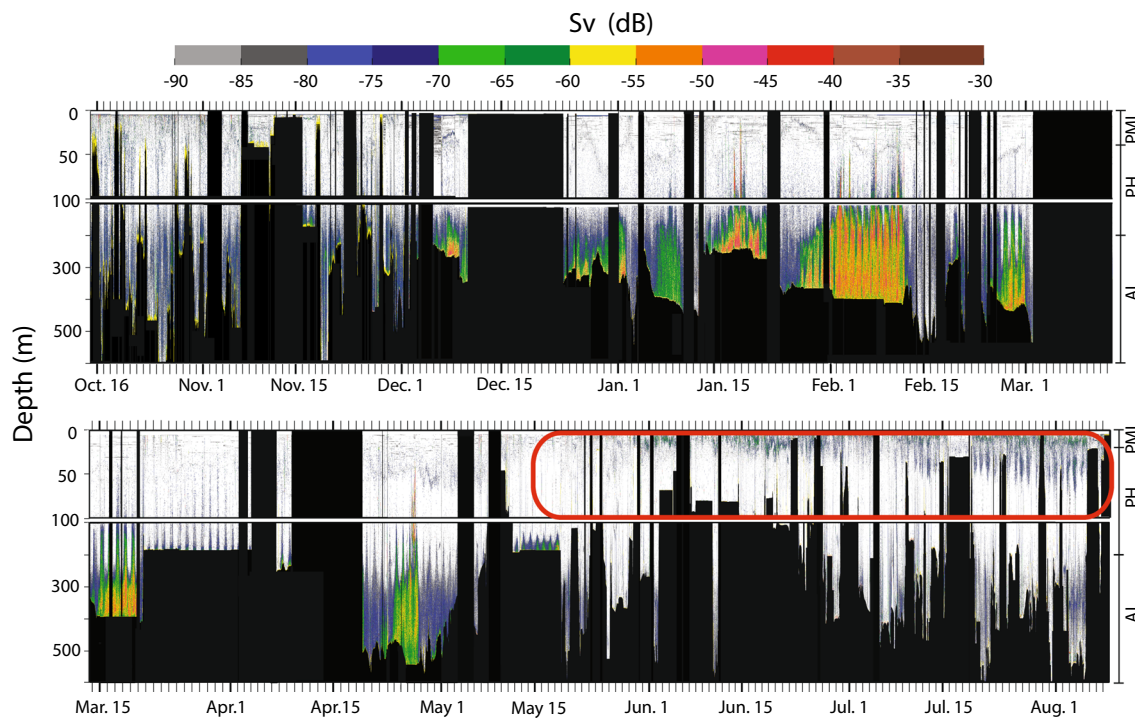


Fig. 3 S_v at 38 kHz during the overwintering expedition of the *Amundsen* from 15 October 2007 to 8 August 2008. Note the different depth scales for the 0- to 100-m and 100- to 600-m layers. Areas below the bottom or with no acoustic data are in black. Each tick on the time axis corresponds to noon local time. The approximate depth

of the Polar-Mixed Layer (PML), Pacific Halocline (PH), and Atlantic Layer (AL) in winter and summer is indicated to the right. The red outline indicates the epipelagic scattering layer of age-0 polar cod in summer

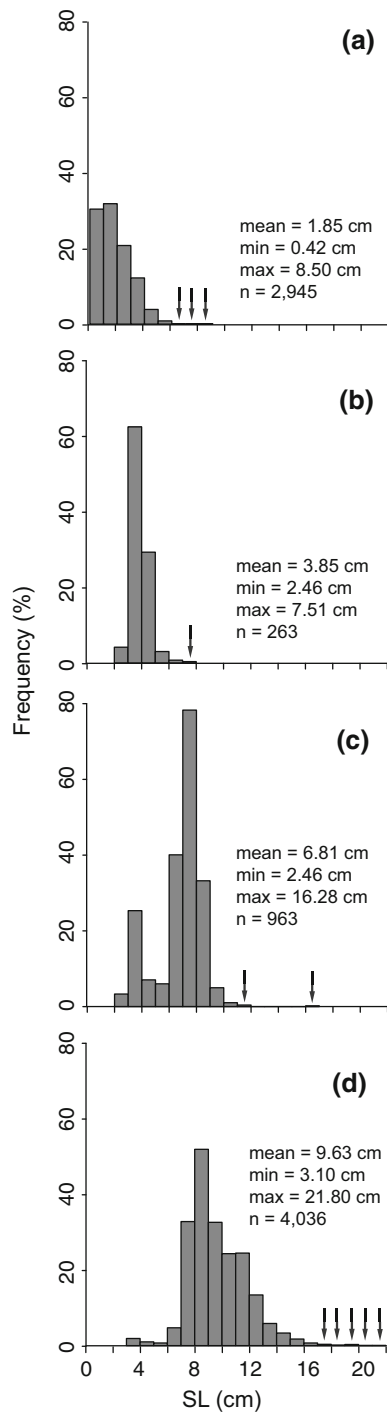


Fig. 4 SL frequency distribution of measured polar cod sampled with **a** ichthyoplankton nets; **b** mid-water trawls in the epipelagic layer (<100 m); **c** mid-water trawls in the mesopelagic layer (200–420 m); and **d** demersal trawls deployed over bottom depths from 200 to 600 m. Black arrows indicate frequencies from >0 to 0.5 %

The mesopelagic layer of age-1+ polar cod persisted year round. The fish were distributed from ~100 m to the seafloor in winter and at depths >200 m in other seasons (Fig. 3). The echo of the mesopelagic layer increased

progressively from December onward to reach a maximum over January–February–March and then declined in May (Fig. 3). Age-1+ polar cod performed DVM within the deep AL from the end of August until mid-May.

The fisheries sonar did not detect a shoal or school of fish in the surface layer over 1418 km of survey in August–September 2011. On seven occasions, dense shoals were observed ascending into the PML when age-1+ polar cod formed a dense mesopelagic layer in January and February 2008 (see Online Resource 4 for an example).

Fish-tracking algorithm versus Sawada Index

Mean TS calculated by the fish-tracking algorithm were slightly lower than by the Sawada Index: –58.8 versus –57.7 dB, respectively, from 13 to 19 March 2008, and –56.4 versus –54.4 dB from 7 to 13 August 2012. Pooling the 2 weeks, the fish-tracking algorithm identified 70,151 single targets compared to 2,606,658 using the Sawada Index.

The vertical distribution of TS and acoustically estimated fish size by month

The logarithmic regression of TS (dB) on SL (cm) explained 55 % of the variance in TS (Eq. 1 and Fig. 5).

$$TS = 14.33 \log_{10}(SL) - 65.13 \quad (1)$$

Between 1 and 5 cm SL, the sampled locations tended to cluster above or below the regression line (Fig. 5). For a given length, the mean time of day, sampling date, and sampling depth were not significantly different between both clusters, suggesting that clustering was unrelated to these variables (Wilcoxon signed-rank test; $p > 0.17$).

Polar cod were vertically segregated by size throughout the year, with TS, and hence SL, increasing from the surface to depth (Fig. 6). Typically in a given month, the average TS was minimum (<–55 dB) in the epipelagic layer (0–100 m), increased with depth over the 100- to 400-m interval to reach maximum values below 400 m (Fig. 6). From April to July, the mean TS near the surface (0–50 m) was –65.1 dB ($n = 191,085$), which corresponded to 1-cm-long polar cod (Eq. 1). From July to September, mean TS in the 0- to 50-m depth interval increased to –55.3 dB ($n = 49,854$, corresponding SL = 4.9 cm) and declined progressively thereafter. Except in July, when the mean TS remained below –51.8 dB, relatively large polar cod (mean TS = –48.23 dB, $n = 22,006$, corresponding SL = 15 cm) were detected below ~300 m from April to January (Fig. 6). Mean TS below 300 m was –50.1 dB ($n = 5471$, corresponding SL = 11.2 cm) in February. Despite strong aggregations at depth in March (Fig. 3), only a few single TS corresponding to

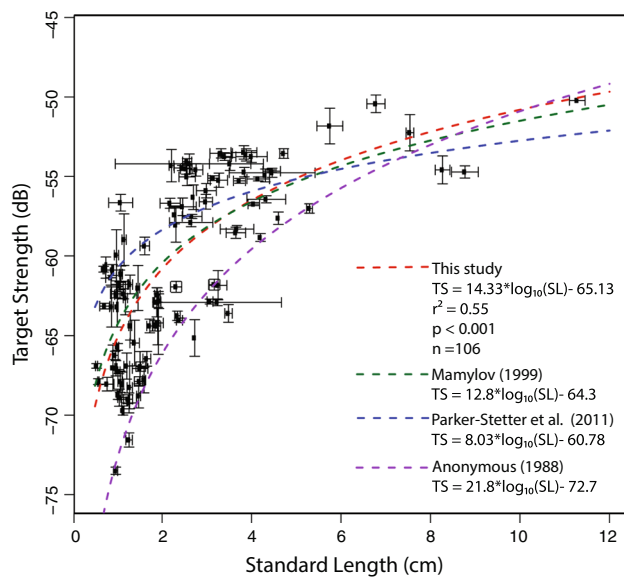


Fig. 5 Regression of the mean TS of single targets detected in the area sampled by ichthyoplankton nets or mid-water trawls on the mean SL of polar cod in the net/trawl collections (see “Materials and methods”). Error bars give the standard error. Regression lines used in previous studies are presented for comparison

small fish were obtained below 300 m (mean TS = -55.7 dB, $n = 12$, corresponding SL = 4.6 cm).

For 50-m depth strata, mean TS for the months of July, August, September, and October did not differ significantly between years ($p > 0.05$) despite different sampling areas and local fish densities, confirming that the data could be pooled by month. Results from the ANOVA and the Kruskal–Wallis test concurred.

The vertical distribution of estimated polar cod biomass over the annual cycle

The power regression of W (g) on SL (cm) for 5860 polar cod was (Fig. 7):

$$W = 0.0055 (SL)^{3.19} \quad (2)$$

From December to March, most of the biomass was concentrated in a relatively shallow mesopelagic layer from 200 to 400 m (Fig. 8). From April to July, the mesopelagic layer deepened and extended to the seafloor at 600 m (Fig. 8). Starting in August and until November, deeper regions were surveyed and some biomass was detected between 600 m and the bottom. A secondary peak in biomass developed in July in the epipelagic layer at depth <200 m and persisted until September before disappearing in October, as the biomass within the mesopelagic layer started increasing.

Except in April, the vertically integrated biomass of age-1+ in the mesopelagic layer was low (4.7 to 26.1 g m⁻²) from February to September (Fig. 8). Biomass was

relatively high (69.6–96.8 g m⁻²) from October to January and in April. The biomass of age-0 in the epipelagic layer (0–100 m) increased from June (0.06 g m⁻²) to September (2.38 g m⁻²) and then decreased over October–January to nearly zero values from January until May (Fig. 8).

Discussion

Acoustical estimates of polar cod size and biomass

Polar cod largely dominate the assemblage of pelagic fish in the Beaufort Sea (e.g. 97 %, Benoit et al. 2008; 99 %, Parker-Stetter et al. 2011). In the present study, sampling by plankton nets and mid-water trawls confirmed that age-0 polar cod made up the vast majority (94 %) of fish in the epipelagic scattering layer. The mesopelagic layer was sampled by mid-water trawl at only 13 locations on the Mackenzie shelf and slope in 2012, but the catch composition was similar to earlier reports (Benoit et al. 2008; Parker-Stetter et al. 2011; Fortier et al. 2015), with age-1+ polar cod strongly dominating the fish assemblage (95 %) followed by similar-sized snailfish and sculpins. We conclude that polar cod made up ~95 % of the pelagic fish detected by acoustics throughout the years and regions surveyed.

A lower mean TS (by 1.1 dB in March and 2 dB in August) and 37-fold fewer single detections indicated that the fish-tracking algorithm was at least as efficient as the Sawada Index approach at eliminating multiple target detections. Using the fish-tracking algorithm with a similar parameterization as in Benoit et al. (2014) likely limited multiple target detections, but perhaps at the potential cost of eliminating some of the larger polar cod from the analysis. Thus, the polar cod biomasses presented here based on mean TS are deemed conservative. Crawford and Jorgensen (1996) observed acoustic shading within dense (up to 307 fish m⁻³) polar cod schools. In the present study, fish density within aggregations remained <35 fish m⁻³ and acoustic shading was probably negligible. TS from single targets were available only from the periphery of the denser winter aggregations, which may or may not be representative of the TS within the aggregations. Admittedly, our estimates of the biomass of these winter aggregations could be biased one way or the other.

A high signal-to-noise ratio (SNR) is required for reliable TS measurements, but the SNR diminishes with depth due to the amplification of noise by the TVG. Hence, the TS detection threshold increases with depth (Kieser et al. 2005). Variations in local sound absorption, background noise levels, and SNR conditions can significantly affect the TS detection threshold. For instance, polar cod <2.3 cm were not detected beyond 200 m when background noise

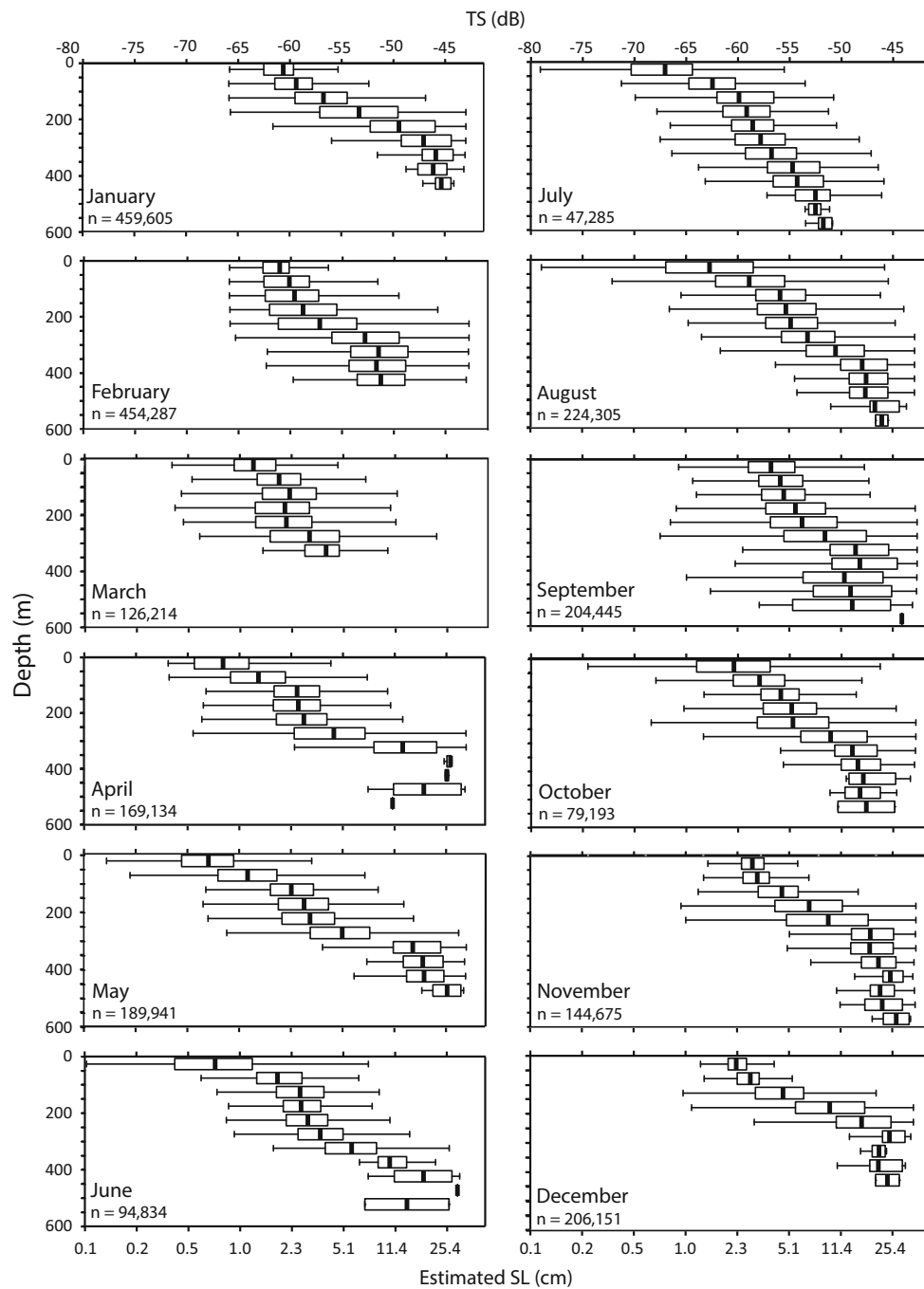


Fig. 6 Box-and-whisker plots of the TS (*top x-axis*) of polar cod by month and by 50-m-deep intervals. The *black vertical line* is the mean, the left and right boundaries of the box are the 25 and 75 percentiles, and the whiskers are the 0 and 100 percentiles. *n* indicates

the number of single targets identified by the fish-tracking algorithm. The *lower x-axis* provides the SL of polar cod corresponding to TS based on Eq. 1

level was -156 dB re: 1 m^2 at 1 m (-60 dB; Online Resource 5 and Eq. 1). The elimination of smaller targets at depth resulted in a bias that could partly explain the increase in mean TS with depth (Fig. 6) and possibly resulted in an overestimation of SL and biomass in the mesopelagic layer. Using similar methods, Benoit et al.

(2014) conducted TS measurements on polar cod down to 500 m and large polar cod were increasingly frequent with depth in trammel nets deployed under the ice in the winter of 2004 (Benoit et al. 2008). In the present study, less than 5 % of the fish captured in the mesopelagic layer were <2.5 cm and the mean SL of the polar cod captured in the

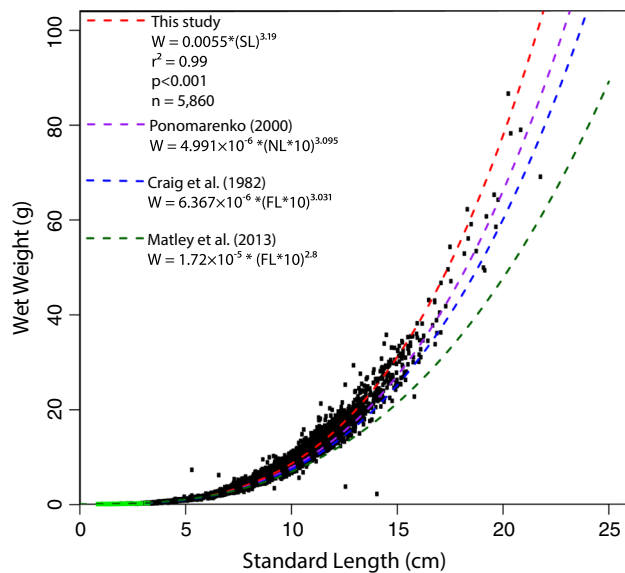


Fig. 7 Regression of wet weight (W) on standard length (SL) for polar cod sampled from 2006 to 2012 (black dots) and in 2013 (green dots). Regressions of polar cod W on notochord length (NL) or fork length (FL) used in previous studies are indicated for comparison

21 mid-water trawl deployments significantly increased with sampling depth from near the surface to 400 m ($0.00938 \times \text{Depth} + 3.48$, $r^2 = 0.75$, $p < 0.001$; Online Resource 6). We thus conclude that, notwithstanding the uncertainties inherent to hydroacoustic estimates of fish size and biomass at depth, the increase in fish size with depth measured acoustically is real and not solely an artefact caused by discarding smaller targets or by more frequent multiple detections. At depths >600 m, the SNR was likely too low to allow single-target detections and the uncertainties in biomass estimates were consequently higher. Moreover, areas deeper than 600 m were only surveyed from August to November, which prevented documenting the complete annual cycle of biomass at these depths.

Avoidance of sampling gears by the largest polar cod could explain the significantly lower biomass derived from the trawls (W. Walkusz; unpublished data) compared to acoustic biomass estimates. Hence, the importance of complementing biomass estimates based on trawls with acoustic estimates based on the relationship between TS and fish length (Williams et al. 2015). Different regressions of TS on length have been used to estimate polar cod biomass (Anonymous 1988; Mamylov 1999; Parker-Stetter et al. 2011). In the present study, the distribution of polar cod into two nearly monospecific age-segregated layers provided ideal conditions to relate TS and length (Warner et al. 2002). The new regression presented here is based on the insonification of fish during 106 net/trawl deployments (Fig. 5). It explains 55 % of the variation in TS and is very close to the regression calculated by Mamylov (1999). The

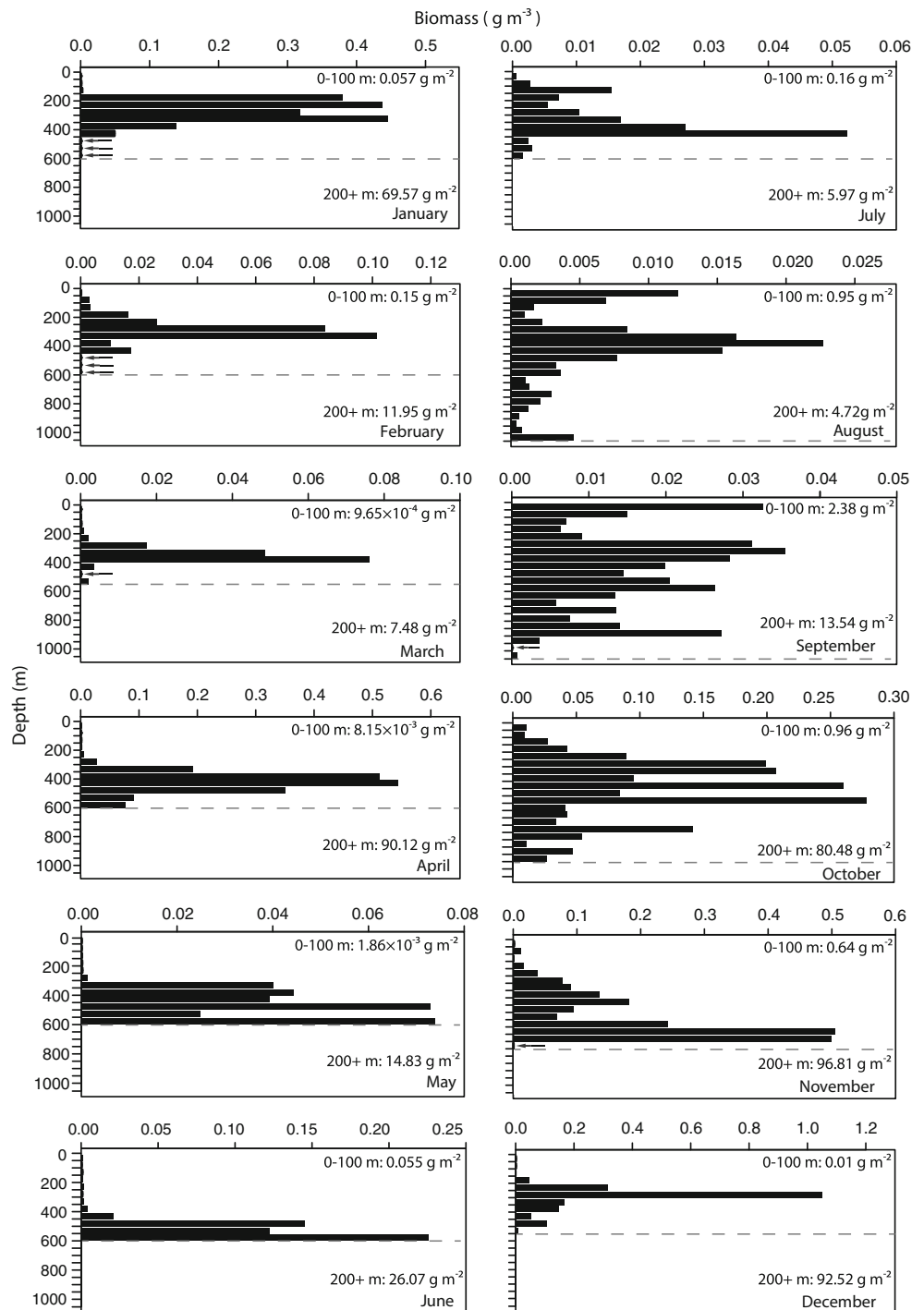
bimodal distribution of variance around the regression curve, with TS-SL points falling either well above or well below the regression, may reflect some bimodal orientation of the fish (head/tail on *versus* top/side on) in the acoustic beam (Gauthier and Horne 2004). Fishing gear avoidance by large individuals and the ensuing underestimation of average length possibly moved the regression curve to the left, resulting in conservative estimates of SL and biomass.

In the epipelagic layer, the ranges of mean TS (-66.1 to -54.4 dB; Fig. 6) and SL estimated from Eq. 1 (0.9–5.6 cm) were consistent with the range of SL of age-0 polar cod sampled by plankton nets in the 0- to 100-m stratum (0.4–8.5 cm, with most fish under 6 cm, Fig. 4a). Interestingly, when polar cod grow from 0.64 to 0.72 cm, the proportion of larvae with an inflated swim bladder increases from 2 to 65 % (Aronovich et al. 1975). Underdeveloped or insufficiently inflated swim bladders may explain that most fish 0.4 to <0.9 cm sampled by plankton nets in the epipelagic layer either escaped detection by the echosounder or were classified as weaker zooplankton targets (Fig. 2), possibly resulting in some underestimation of biomass within the epipelagic layer from May to July. As well, polar cod larvae (average SL = 1.37 cm) concentrate in the 0- to 10-m layer during the summer months (Bouchard et al. in press) and the acoustic blind zone over the top 13.5 m certainly contributed to underestimating the epipelagic biomass of age-0 fish. Otherwise, the similarity of the SL ranges estimated by nets and acoustics for the epipelagic layer suggests that plankton nets efficiently sampled young fish and that the proposed TS-SL regression is accurate for age-0 polar cod.

The polar cod sampled in August and early September by mid-water trawls in the mesopelagic layer were smaller (mean SL = 6.8 cm) than the average length in August estimated acoustically for that layer (mean TS = -51.3 dB, corresponding SL = 9.2 cm), suggesting trawl avoidance. Polar cod caught in demersal trawls deployed in the same region in 2012 were larger than in the mid-water trawls (Fig. 4c, d), indicating that bigger individuals remained near the seafloor, thus avoiding the mid-water trawls.

Previous regressions of polar cod weight on notochord length (NL, Ponomarenko 2000) or fork length (FL, Craig et al. 1982; Matley et al. 2013) have been published. All these equations, including the one in this study, yield similar weight for fish <10 cm (Fig. 7). The Ponomarenko (2000) W -NL equation for Barents, Kara, and White Seas polar cod generally underestimates the weight of Beaufort Sea fish in the range 10–15 cm, while our equation overestimates weight in fish >15 cm. The W -FL regressions reported by Craig et al. (1982) for the American Beaufort Sea and by Matley et al. (2013) for the Canadian Archipelago underestimate the weight of Canadian Beaufort Sea

Fig. 8 Biomass of polar cod (g m^{-3}) averaged per month and 50-m depth intervals. Integrated biomass (g m^{-2}) in the epipelagic (0–100 m) and mesopelagic (200+ m) layers is also indicated. Note the different biomass scales in different months. *Black arrows* point to depth intervals where biomass was close to zero. The *stippled horizontal line* indicates the maximum depth surveyed in a given month (± 50 m)



polar cod at length >10 cm (Fig. 7). Some of the discrepancy may stem from their measurement of FL rather than the shorter SL used here.

The vertical distribution of polar cod length and biomass over the year in the Beaufort Sea

At a 230-m-deep station in the landfast ice of Franklin Bay (Fig. 1), the progressive build-up of a dense aggregation of

polar cod over winter months resulted in vertically integrated biomasses reaching 55 kg m^{-2} in April (Benoit et al. 2008). By comparison, biomass within winter aggregations of polar cod over the slope attained a maximum of no more than 0.732 kg m^{-2} in February (Geoffroy et al. 2011). Both studies focused on peak biomass within dense winter aggregations and used the TS to length regression of Anonymous (1988), which, according to our results, overestimates the length of polar cod (Fig. 5).

Aware of these potential limitations, Benoit et al. (2008) emphasized the need to test the validity of the TS analysis, based on in situ measurements with split-beam target-tracking techniques. Using these techniques and new TS-SL and W-SL regressions, we report here much lower biomasses ($0.01\text{--}0.1\text{ kg m}^{-2}$, Fig. 8) averaged by months over regions with and without aggregations.

Benoit et al. (2010) proposed that large polar cod distribute close to the bottom in winter to limit predation by deep-diving mature ringed seals (*Pusa hispida*) that target the lipid-rich livers of the largest fish. Based on photosynthetically active radiation at the surface, Geoffroy et al. (2011) further linked the deepening of the distribution of polar cod from December to April to the vernal increase in irradiance that provides visual predators such as ringed seals and belugas (*Delphinapterus leucas*; see Asselin et al. 2011) with increasing light to catch polar cod at depth. We suspect that from February to September, with the exception of April, most large polar cod remained near the seafloor to avoid marine mammal predators and were distributed too close to the bottom for the echosounder to detect them, resulting in low monthly biomass estimates. This is confirmed for February, March, and July when the TS of fish in the insonified water column diminished (Fig. 6). With rapidly declining irradiance and vulnerability to visual predators in September–October, large polar cod left the seafloor (Fig. 6), resulting in large biomasses being detected by the echosounder in the mesopelagic layer (Fig. 8). This colonization of the AL in September–October coincided with the descent of the large CV stages and females of *C. hyperboreus* to depths $>200\text{ m}$ at the end of summer (Darnis and Fortier 2014). Of course, other factors may have contributed to variations in monthly estimates of biomass, such as the frequency of encounters with aggregations along the ship track, the dense congregation of large fish that can prevent their detection by the fish-tracking algorithm, and the depth of the region surveyed in a given month.

Consistent with the hypothesis of Geoffroy et al. (2011), the intriguing peak in biomass in April (Fig. 8) could be linked to large polar cod leaving their seafloor habitat to pursue *C. hyperboreus* and *C. glacialis* prey as they ascend from the deep Atlantic Layer (AL) and Pacific Halocline (PH) towards the Polar-Mixed Layer (PML) (Darnis and Fortier 2014). Some age-1+ were seen rising briefly into the epipelagic layer in late April, possibly due to predation by larger congeners or marine mammals within the aggregations, but otherwise no significant concentrations of adult polar cod were detected above 100 m in spring–summer (Fig. 3). As well, only nine age-1 and no age-2+ were captured in the 8 mid-water trawls deployed in the epipelagic layer (0–65 m) in August and early September. Finally, no schooling adults were detected in

the surface layer by the SX90 fisheries sonar over the 1418 km surveyed from August to October 2011 across bottom depths ranging from 20 to $>1000\text{ m}$. Hence, the brief excursion of age-1+ in the epipelagic layer in late April differed little from similar events linked to the DVM of polar cod in winter months (Fig. 3), and there was no indication that the large polar cod briefly leaving the bottom in April reached the PML and remained therein during the spring and summer months. We conclude that age-1+ polar cod seldom move into the offshore epipelagic layer over the annual cycle.

The fall migration of age-0 polar cod to depth

In the Barents Sea region, age-0 polar cod 3.5–5.0 cm in length descended to deeper levels in August–September but remained in the water column until late September (Ponomarenko 2000). Age-0 started to occur in the near-bottom layers with increasing frequency in November and December. In the present study, clear DVM started in mid-July–early August in the epipelagic layer (Fig. 3, red outline), when TS within the 50- to 100-m stratum reached roughly -58 dB , corresponding to polar cod 3 cm long that became fully motile after metamorphosis. In September and October, the amplitude of the DVM increased, and age-0 with a TS of -54.5 dB (5.5 cm) progressively joined their conspecifics in the PH (see the echogram in Online Resource 3). As observed in the Barents Sea region (Ponomarenko 2000), the biomass of migrating age-0 in the epipelagic layer peaked in September (Fig. 8). According to the length–age relationship $SL_{\text{mm}} = 9.353 + 0.182\text{ age}_{\text{days}}$ ($r^2 = 0.803$, $n = 102$, Bouchard and Fortier 2011), these 3- to 5.5-cm SL polar cod were 113–251 d old in September and their hatching period, from January to May, agrees with previous reports (Bouchard and Fortier 2011, Bouchard et al. in press).

Age-0 polar cod $>2.5\text{ cm}$ obtain 92 % of their carbon uptake from copepodite prey (primarily *C. hyperboreus*, *C. glacialis*, *Metridia longa*, and *Pseudocalanus* spp.), and prey size increases with fish length (Falardeau et al. 2014). As they grow in late summer and fall, age-0 polar cod in the epipelagic layer become increasingly conspicuous to seabird predators (Sogard 1997; Matley et al. 2012). The clear DVM exhibited from August to October indicate that age-0 polar cod fed in the surface layer at night and descended in daytime to avoid visual predators. As the surface layer emptied of copepod prey in November, with, for instance, the density of *C. hyperboreus* decreasing to $<5\text{ ind m}^{-3}$ (Darnis and Fortier 2014), the DVM blurred and age-0 remained at depth (Online Resource 3). Hence, as prey abundance declines and vulnerability to visual predators increases, the changing balance of risk against benefits for a growing age-0 polar cod likely triggers the

end of the DVM and the onset of the ontogenetic migration out of the epipelagic layer.

Several studies have documented the presence of polar cod <2 years of age in sea ice anfractuositities, indicating that some individuals are sympagic early in the life cycle (e.g. Lønne and Gulliksen 1989; Gradinger and Bluhm 2004; Melnikov and Chernova 2013). However, our results show that the majority of age-0 hatched in the epipelagic layer in winter and spring (January–May) had descended into the PH and AL at depths >100 m by the end of October (Fig. 8). The residual biomass (0.64 g m^{-2}) of age-0 in the epipelagic layer in November that soon disappeared in December (0.01 g m^{-2}) would correspond to late hatchers in June and early July (Bouchard and Fortier 2011; Bouchard et al. in press). The decreasing mean TS within the epipelagic layer in the fall (Fig. 6) supports the idea that while large early hatchers descended to deeper layers, small late hatchers remained in the surface layer. We hypothesize that these late hatchers recruit to the ice cover as the ice consolidates in November and later descend to the AL to join the mesopelagic fish layer once the ice starts to melt in summer. The highly variable surface circulation and the eastward Beaufort shelf-break jet often carry ice flows over the shelf and in the shallow Canadian Archipelago (Carmack and Macdonald 2002; Pickart 2004). As this ice melts in summer, ice-associated polar cod would become pelagic, possibly forming the schools and shoals detected in coastal areas of the inner shelf and Archipelago (Crawford and Jorgenson 1993; Welch et al. 1993; Parker-Stetter et al. 2011; Matley et al. 2013). Advection of the buoyant eggs or planktonic larvae and juveniles in shallow areas (Melnikov and Chernova 2013), before their descent in autumn, may also contribute to coastal schools. Such mechanisms would explain the ubiquitous but sparsely distributed immature age-1+ polar cod over the Canadian Beaufort Sea shelf (Majewski et al. 2013; Walkusz et al. 2013). Young polar cod dispersed in shallow areas would migrate offshore after reaching sexual maturity at age 2 or 3 (Craig et al. 1982) where they would join the mesopelagic fish layer in the AL to reproduce.

The vertical segregation of polar cod by size in the Beaufort Sea

In winter in Franklin Bay, age-1+ polar cod were distributed in the lower PH from 140 m to the bottom at 230 m, in waters corresponding to slope water (Benoit et al. 2008). Relatively small fish (11.6–15 cm, 4–25 g) spanned the entire 140- to 225-m interval, whereas longer and heavier fish (15–25.5 cm, 25–95 g) were found only at depth >180 m, increasing in number with depth (Benoit et al. 2010). Our results confirm that polar cod distribute deeper in the PH and the AL with increasing size. In

addition, the resolution achieved with acoustical estimates of TS illustrates the remarkable vertical segregation of polar cod by size over the entire annual cycle (Fig. 6). The regular increase in TS with depth in all months indicates that for most polar cod, the migration from the epipelagic layer to the near-bottom AL is a protracted process unfolding over the first several years of the 7-year lifespan. Such progressive ontogenetic migration results in a clear segregation of the age/size classes over depth (Fig. 6). The vertical co-occurrence of fish of roughly the same length in a given depth strata would strongly limit cannibalism, a conclusion consistent with the observation that fish represent less than 8 % of the diet of pelagic polar cod (Rand et al. 2013).

Implications: the vulnerability of polar cod to longer ice-free seasons and potential oil spills in the offshore Beaufort Sea

Over the past decade, the Beaufort Sea ecosystem has experienced an extension of the ice-free seasons, with ice break-up as early as May and ice pack consolidation in November or December (Markus et al. 2009; Stroeve et al. 2012). The increased solar irradiation of the surface waters resulted in higher sea-surface temperatures in spring and summer (Wood et al. 2013), during the growth season of age-0 epipelagic polar cod. Warmer temperature accelerates the growth of polar cod larvae and juveniles (Bouchard and Fortier 2011), which can improve recruitment (e.g. Pörtner et al. 2001). Longer ice-free seasons may also result in increased predation of the epipelagic larvae and juveniles by sea birds. Based on the present results, we would predict that climate-induced modification of the ice and temperature regimes in the surface layer will impact first and most directly the epipelagic larval and juvenile stages of polar cod, their planktonic food, and their predators. While age-0 and age-1+ inhabiting the ice cover and the inner shelf and Archipelago (Crawford and Jorgenson 1993; Welch et al. 1993; Parker-Stetter et al. 2011; Matley et al. 2013) would also be impacted, polar cod occupying the mesopelagic layer offshore would be less affected.

Offshore exploration for oil in the Canadian Arctic Ocean targets the shelf break and slope of the Beaufort Sea where lease blocks have been awarded in 2007. Hydrocarbons at concentrations typical of those measured in areas affected by a spill depress the routine metabolism of polar cod, induce DNA damage, and can be lethal (e.g. Christiansen et al. 2010; Nahrgang et al. 2010). Age-0 polar cod in the epipelagic layer are widely distributed on and off the Mackenzie shelf (M. Geoffroy, unpublished data). Based on modelling studies, oil spilled at the surface or raising to the surface from a point source on the slope in

summer could propagate in the Amundsen Gulf eastward and over much of the Canadian and US Beaufort Sea to the west (Schroeder Gearon et al. 2014), potentially impacting age-0 polar cod over much of its distribution.

Observations and modelling studies indicate that the injection of dispersant in the oil raising from a well blow-out at the seafloor can result in the horizontal dispersion of a plume of highly toxic dispersant/oil bubbles that can remain trapped at depth for years (e.g. Paris et al. 2012; Dietrich et al. 2014). In the offshore Beaufort Sea, such a plume propagating in the 200- to 400-m interval from December to June would expose age-1+ polar cod to dispersed hydrocarbons for several months. From August to November, the mesopelagic polar cod would be vulnerable to plumes in the 200–800 + m interval (Fig. 8). Coupled biological–physical models incorporating the ontogenetic changes in the vertical distribution reported here are needed to anticipate the impacts of longer ice-free seasons and potential oil spill scenarios on polar cod and its ecosystem.

Acknowledgments We thank the officers and crew of the CCGS *Amundsen* and F/V *Frosti* for their dedication and professionalism. The calibration of the echosounder in 2012 was conducted with the help of George Cronkite at the Pacific Biological Station (DFO). Several technicians and colleagues contributed to sample collection from 2006 to 2012. Special thanks to Jane Eert and Mike Dempsey (DFO) for technical support on board the *Frosti*, to Shani Rousseau and Dominique Robert (Université Laval) for preliminary analysis, and to Yvan Simard (DFO) for advice during calibration and operation of the *Amundsen*'s echosounder. This manuscript benefited from the constructive comments of four anonymous reviewers and two editors. The National Oceanic and Atmospheric Administration graciously lent the transducers used during the 2012 survey. This is a contribution to Québec-Océan at Université Laval, ArcticNet, and the Canada Research Chair on the Response of Arctic Marine Ecosystems to Climate Change.

Funding Aboriginal Affairs and Northern Development Canada (Beaufort Region Environmental Assessment program), ArcticNet, and Fisheries and Oceans Canada provided financial support. Imperial Oil Resources Ventures Limited and BP Exploration Operating Company Limited partly funded ship time from 2009 to 2011. MG benefited from scholarships from the Natural Sciences and Engineering Research Council of Canada and the W. Garfield Weston foundation.

Compliance with ethical standards

Conflict of interest The authors declare that they have no conflict of interest.

Ethical approval All applicable international, national, and institutional guidelines for the care and use of animals were followed. This active acoustics research project was reviewed by the Environmental Impact Screening Committee (EISC) for the Inuvialuit Settlement Region (www.screeningcommittee.ca). Following the reviews, scientific research licences were issued by the Aurora Research Institute in accordance with the Northwest Territories Scientists Act.

References

- Anonymous (1988) Report on the joint Norwegian/USSR acoustic survey of pelagic fish in the Barents Sea, September–October 1988. Institute of Marine Research, Bergen
- Aronovich TM, Doroshev SI, Spectorova LV, Makhotin VM (1975) Egg incubation and larval rearing of Nagava (*Eleginus nagava* Pall.), Polar cod (*Boreogadus saida* Lepechin), and Arctic flounder (*Liopsetta glacialis* Pall.) in the laboratory. *Aquacult* 6:233–242
- Asselin N, Barber D, Stirling I, Ferguson S, Richard P (2011) Beluga (*Delphinapterus leucas*) habitat selection in the eastern Beaufort Sea in spring, 1975–1979. *Polar Biol* 34:1973–1988
- Benoit D, Simard Y, Fortier L (2008) Hydroacoustic detection of large winter aggregations of Arctic cod (*Boreogadus saida*) at depth in ice-covered Franklin Bay (Beaufort Sea). *J Geophys Res Ocean* 113:C06S90
- Benoit D, Simard Y, Gagne J, Geoffroy M, Fortier L (2010) From polar night to midnight sun: photoperiod, seal predation, and the diel vertical migrations of polar cod (*Boreogadus saida*) under landfast ice in the Arctic Ocean. *Polar Biol* 33:1505–1520
- Benoit D, Simard Y, Fortier L (2014) Pre-winter distribution and habitat characteristics of polar cod (*Boreogadus saida*) in southeastern Beaufort Sea. *Polar Biol* 37:149–163
- Bouchard C, Fortier L (2011) Circum-arctic comparison of the hatching season of polar cod *Boreogadus saida*: a test of the freshwater winter refuge hypothesis. *Prog Oceanogr* 90:105–116
- Bouchard C, Mollard S, Suzuki K, Robert D, Fortier L (in press) Contrasting the early life histories of sympatric Arctic gadids *Boreogadus saida* and *Arctogadus glacialis* in the Canadian Beaufort Sea. *Polar Biol*, this volume
- Carmack EC, Macdonald RW (2002) Oceanography of the Canadian Shelf of the Beaufort Sea: a setting for marine life. *Arctic* 55:29–45
- Christiansen JS, Karamushko L, Nahrgang J (2010) Sub-lethal levels of waterborne petroleum may depress routine metabolism in polar cod *Boreogadus saida* (Lepechin, 1774). *Polar Biol* 33:1049–1055
- Craig PC, Griffiths WB, Haldorson L, McElderry H (1982) Ecological Studies of Arctic Cod (*Boreogadus saida*) in Beaufort Sea Coastal Water. *Can J Fish Aquat Sci* 39:395–406
- Crawford RE, Jorgenson JK (1993) Schooling behaviour of arctic cod, *Boreogadus saida*, in relation to drifting pack ice. *Environ Biol Fish* 36:345–357
- Crawford RE, Jorgenson JK (1996) Quantitative studies of Arctic cod (*Boreogadus saida*) schools: important energy stores in the Arctic food web. *Arctic* 49:181–193
- Crawford R, Vagle S, Carmack EC (2012) Water mass and bathymetric characteristics of polar cod habitat along the continental shelf and slope of the Beaufort and Chukchi seas. *Polar Biol* 35:179–190
- Darnis G, Fortier L (2014) Temperature, food and the seasonal vertical migration of key arctic copepods in the thermally stratified Amundsen Gulf (Beaufort Sea, Arctic Ocean). *J Plankton Res* 36:1092–1108
- David C, Lange B, Krumpfen T, Schaafsma F, van Franeker JA, Flores H (in press) Under-ice distribution of polar cod *Boreogadus saida* in the Central Arctic Ocean and their association with sea-ice habitat properties. *Polar Biol*, this volume
- Dietrich DE, Bowman MJ, Korotenko KA, Bowman MHE (2014) Oil spill risk management: modeling Gulf of Mexico circulation and oil dispersal. Wiley, New York
- Falardeau M, Robert D, Fortier L (2014) Could the planktonic stages of polar cod and Pacific sand lance compete for food in the warming Beaufort Sea? *ICES J Mar Sci* 71:1956–1965

- Footo KG (1987) Fish target strengths for use in echo integrator surveys. *J Acoust Soc Am* 82:981–987
- Fortier L, Ferguson SH, Archambault P, Matley J, Robert D, Darnis G, Geoffroy M et al. (2015) Arctic change: impacts on marine ecosystems. In: Stern G, Gaden A (eds) From science to policy in the western and central Canadian Arctic. ArcticNet Inc., Quebec City
- Francois RE, Garrison GR (1982) Sound-absorption based on ocean measurements. 2. Boric-acid contribution and equation for total absorption. *J Acoust Soc Am* 72:1879–1890
- Gauthier S, Horne JK (2004) Potential acoustic discrimination within boreal fish assemblages. *ICES J Mar Sci* 61:836–845
- Gauthier S, Rose GA (2001) Diagnostic tools for unbiased in situ target strength estimation. *Can J Fish Aquat Sci* 58:2149–2155
- Geoffroy M, Robert D, Darnis G, Fortier L (2011) The aggregation of polar cod (*Boreogadus saida*) in the deep Atlantic layer of ice-covered Amundsen Gulf (Beaufort Sea) in winter. *Polar Biol* 34:1959–1971
- Geoffroy M, Rousseau S, Knudsen FR, Fortier L (2015) Target strengths and echotracers of whales and seals in the Canadian Beaufort Sea. *ICES J Mar Sci*. doi:10.1093/icesjms/fsv182
- Gradinger RR, Bluhm BA (2004) *In-situ* observations on the distribution and behavior of amphipods and Arctic cod (*Boreogadus saida*) under the sea ice of the High Arctic Canada Basin. *Polar Biol* 27:595–603
- Kieser R, Reynisson P, Mulligan TJ (2005) Definition of signal-to-noise ratio and its critical role in split-beam measurements. *ICES J Mar Sci* 62:123–130
- Lønne OJ, Gulliksen B (1989) Size, age and diet of polar cod, *Boreogadus saida* (Lepechin 1773) in ice covered waters. *Polar Biol* 9:189–191
- Mackenzie KV (1981) Nine-term equation for sound speed in the oceans. *J Acoust Soc Am* 70:807–812
- Majewski AR, Lynn BR, Lowdon MK, Williams WJ, Reist JD (2013) Community composition of demersal marine fishes on the Canadian Beaufort Shelf and at Herschel Island, Yukon Territory. *J Mar Syst* 127:55–64
- Mamylov VS (1999) Some aspects of estimating the density of fish aggregations by trawl-acoustic methods. Development of technical methods for fisheries research. PINRO selected papers, Murmansk, Russia, pp. 147–163 (In Russian)
- Markus T, Stroeve JC, Miller J (2009) Recent changes in Arctic sea ice melt onset, freeze up, and melt season length. *J Geophys Res Oceans* 114:C12024
- Matley JK, Fisk AT, Dick TA (2012) Seabird predation on Arctic cod during summer in the Canadian Arctic. *Mar Ecol Prog Ser* 450:219–228
- Matley J, Fisk A, Dick T (2013) The foraging ecology of Arctic cod (*Boreogadus saida*) during open water (July–August) in Allen Bay, Arctic Canada. *Mar Biol* 160:2993–3004
- McLaughlin F, Carmack EC, Proshutinsky A, Krishfield R, Guay C, Yamamoto-Kawai M, Jackson J, Williams B (2011) The rapid response of the Canada Basin to climate forcing: from bellwether to alarm bells. *Oceanography* 24:146–159
- Mecklenburg CW, Peter Rask Møller P, Steinke D (2011) Biodiversity of arctic marine fishes: taxonomy and zoogeography. *Mar Biodiv* 41:109–140
- Melnikov IA, Chernova NV (2013) Characteristics of under-ice swarming of polar cod *Boreogadus saida* (Gadidae) in the Central Arctic Ocean. *J Ichthyol* 53:7–15
- Nahrgang J, Camus L, Gonzalez P, Jönsson M, Christiansen JS, Hop H (2010) Biomarker responses in polar cod (*Boreogadus saida*) exposed to dietary crude oil. *Aquat Toxicol* 96:77–83
- Paris CB, Hénaff ML, Aman ZM, Subramaniam A, Helgers J, Wang DP, Kourafalou VH, Srinivasan A (2012) Evolution of the Macondo Well blowout: simulating the effects of the circulation and synthetic dispersants on the subsea oil transport. *Environ Sci Technol* 46:13293–13302
- Parker-Stetter SL, Rudstam LG, Sullivan PJ, Warner DM (2009) Survey calculations. Standard operating procedures for fisheries acoustic surveys in the Great Lakes. Great Lakes Fishery Commission, Ann Arbor, pp 131–147
- Parker-Stetter SL, Horne JK, Weingartner TJ (2011) Distribution of polar cod and age-0 fish in the US Beaufort Sea. *Polar Biol* 34:1543–1557
- Pickart RS (2004) Shelfbreak circulation in the Alaskan Beaufort Sea: mean structure and variability. *J Geophys Res Ocean* 109:C04024
- Ponomarenko VP (2000) Eggs, larvae, and juveniles of polar cod *Boreogadus saida* in the Barents, Kara, and White Seas. *J Ichthyol* 40:165–173
- Pörtner HO, Berdal B, Blust R, Brix O, Colosimo A, De Wachter B, Giuliani A et al (2001) Climate induced temperature effects on growth performance, fecundity and recruitment in marine fish: developing a hypothesis for cause and effect relationships in Atlantic cod (*Gadus morhua*) and common eelpout (*Zoarces viviparus*). *Cont Shelf Res* 21:1975–1997
- Rand K, Whitehouse A, Logerwell E, Ahgeak E, Hibpshman R, Parker-Stetter S (2013) The diets of polar cod (*Boreogadus saida*) from August 2008 in the US Beaufort Sea. *Polar Biol* 36:907–912
- Rudstam LG, Parker-Stetter SL, Sullivan PJ, Warner DM (2009) Towards a standard operating procedure for fishery acoustic surveys in the Laurentian Great Lakes, North America. *ICES J Mar Sci* 66:1391–1397
- Sawada K, Furusawa M, Williamson NJ (1993) Conditions for the precise measurement of fish target strength *in situ*. *J Mar Acoust Soc Japan* 20:73–79
- Schroeder Gearon M, French McCay D, Chaite E, Zamorski S, Reich D, Rowe J, Schmidt-Etkin D (2014) SIMAP modelling of hypothetical oil spills in the Beaufort Sea for World Wildlife Fund (WWF). RPS ASA, South Kingston
- Simmonds J, MacLennan D (2005) Fisheries acoustics: Theory and practice, 2nd edn. Blackwell Publishing, Oxford 456 pp
- Sogard SM (1997) Size-selective mortality in the juvenile stage of teleost fishes: a review. *Bull Mar Sci* 60:1129–1157
- Stroeve JC, Serreze MC, Holland MM, Kay JE, Malanik J, Barrett AP (2012) The Arctic's rapidly shrinking sea ice cover: a research synthesis. *Clim Change* 110:1005–1027
- Walkusz W, Majewski A, Reist JD (2013) Distribution and diet of the bottom dwelling Arctic cod in the Canadian Beaufort Sea. *J Mar Syst* 127:65–75
- Warner DM, Rudstam LG, Klumb RA (2002) In situ target strength of alewives in freshwater. *Trans Am Fish Soc* 131:212–223
- Welch HE, Bergmann MA, Siferd TD, Martin KA, Curtis MF, Crawford RE, Conover RJ, Hop H (1992) Energy flow through the marine ecosystem of the Lancaster Sound region, arctic Canada. *Arctic* 45:343–357
- Welch HE, Crawford RE, Hop H (1993) Occurrence of Arctic cod (*Boreogadus saida*) schools and their vulnerability to predation in the Canadian High Arctic. *Arctic* 46:331–339
- Williams K, Horne KJ, Punt AE (2015) Examining influences of environmental, trawl gear, and fish population factors on midwater trawl performance using acoustic methods. *Fish Res* 164:94–101
- Wood KR, Overland JE, Salo SA, Bond NA, Williams WJ, Dong X (2013) Is there a “new normal” climate in the Beaufort Sea? *Polar Res* 32:19552